MAX-PLANCK-INSTITUT FÜR PLASMAPHYSIK

GARCHING BEI MÜNCHEN

A Scrape-off Layer Based Density Limit for JET ELMy H-modes

K. Borrass J. Lingertat, R. Schneider

IPP 5/75 September 1997

Presented at the 6th International Workshop
on Plasma Edge Theory in Fusion Devices
Oxford, UK, 1997
(to be published in Contrib. Plasma Phys.)

Die nachstehende Arbeit wurde im Rahmen des Vertrages zwischen dem Max-Planck-Institut für Plasmaphysik und der Europäischen Atomgemeinschaft über die Zusammenarbeit auf dem Gebiete der Plasmaphysik durchgeführt.

A Scrape-off Layer Based Density Limit for JET ELMy H-modes

K. Borrass[1)], J. Lingertat[2)], R. Schneider[1)]

[1)] Max-Planck-Institut für Plasmaphysik, Garching/Munich, Germany

[2)] JET Joint Undertaking, Abingdon, Oxfordshire. United Kingdom

Abstract

During a density ramp-up JET ELMy H-modes typically show a saturation of the core density which may even be followed by a decrease (density limit). At the limit the discharge detaches between ELMs and a recently proposed edge based detachment limit for the separatrix density applies. In this paper a simple picture is proposed for the relation between separatrix and core density which allows us to derive the corresponding limit for the core density. The empirical evidence from JET is discussed and compared with the model predictions. It is shown that the resulting limit for the line averaged density coincides in size and scaling with the empirical Greenwald limit.

1. Introduction

When the density is ramped-up in an ELMy H-mode discharge, the density saturates ore even drops, if the gas rate is further increased (density limit (DL)). During this evolution the ELM frequency increases while confinement continuously degrades. This limit is routinely reached in JET [1]. Figure 1 illustrates position and shape of this boundary in relation to the well known L-H transition threshold and the ballooning limit boundary in the pedestal temperature-pedestal density plane [2].

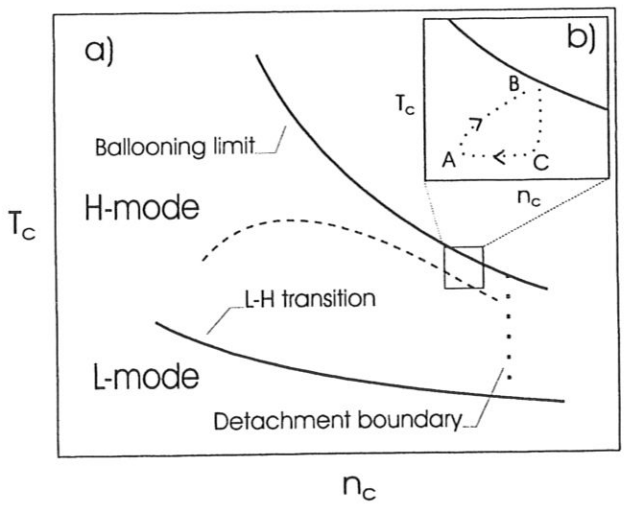

FIG. 1. *(a) Schematic view of H-mode operation boundaries in the pedestal temperature (T_C)-pedestal density (n_C) plane. Also shown is the trajectory of a typical ELMy H-mode density limit discharge (dashed curve, averaged over an ELM period). (b) Trajectory during an ELM period in the type I ELM region (schematic). The ELM starts when the ballooning limit is reached (B). The fast temperature drop (BC) is followed by a density drop (CA). In between ELMs n_C and T_C gradually increase (AB) until the next ELM occurs.*

Experimentally one finds that at the density limit:

(i) $\tau_{ELM} >> \tau_{SOL}$ holds, where τ_{ELM} is the ELM period and τ_{SOL} is the time the scrape-off layer (SOL) needs to reach steady state conditions ($\approx$ 5ms), and, hence, the SOL is in steady state between ELMs.

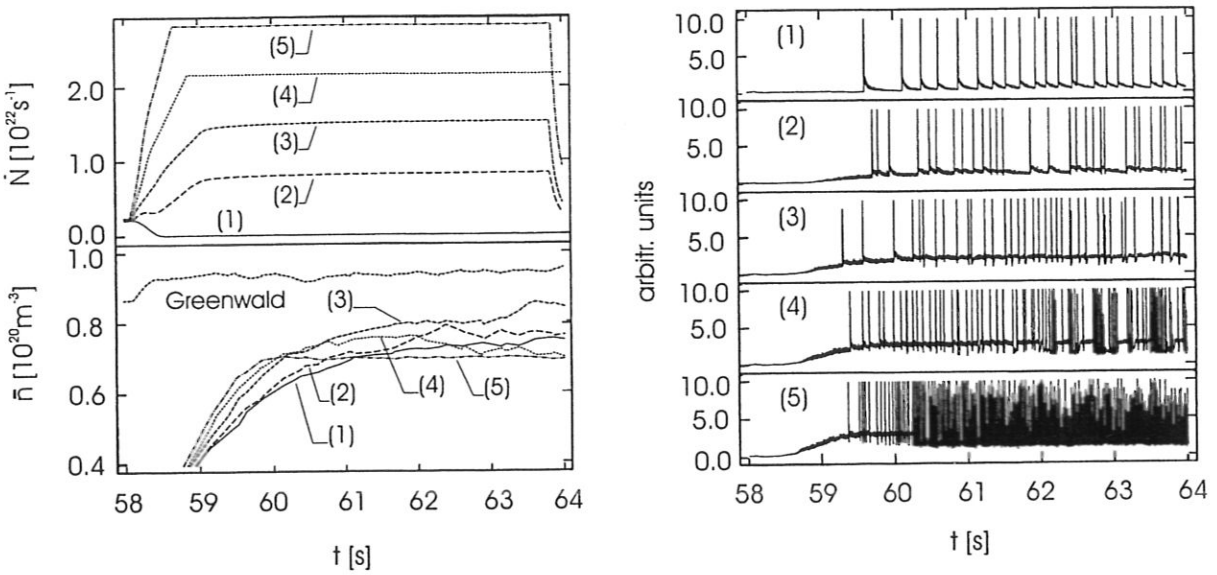

FIG. 2. *Left: time traces of gas rates $\dot{N}$ (upper) and line averaged densities $\bar{n}$ (lower) for a series of ELMy H-mode discharges with increasing gas rate. Right: time traces of the inboard D_α signal for the same series of discharges. When $\bar{n}$ saturates, ELMs are followed by a drop of the D_α signal ("negative ELMs") indicating detachment of the inner divertor.*

(ii) Between ELMs the discharge detaches at the inner divertor.

Under these conditions the SOL based model for the upstream density n_S, proposed in Ref. [3], applies between ELMs and provides information on the maximum achievable separatrix density.

In practice core densities (e.g., line averaged density $\bar{n}$) are also important, since they may be subject to conflicting constraints in next generation devices [4] and enter into most existing density limit databases. While in L-mode $\bar{n}$ and n_S can be relatively successfully related to each other by the simple assumption $\bar{n}/n_S \simeq const$ [5, 6, 3], this approach would be questionable in the case of an H-mode, where the profiles are strongly determined by the physics of the pedestal. On the other hand the density profiles are generally rather flat inside the pedestal in the absence of strong central fuelling, so that $n_C \simeq \bar{n}$, where n_C is the pedestal density. In this paper we propose a simple picture of how to relate n_S and n_C which then allows us to translate the results of Ref. [3] into information on n_C or $\bar{n}$.

The present study strongly relies on details of experimental data. We therefore confine ourselves to the interpretation of JET data where extensive H-mode campaigns have been performed for the MARK-I and II divertor configurations and the material has been produced in a form most suitable for an analysis along the lines of this paper.

2. Experimental Findings

We first discuss evidence for the two conditions (i) and (ii). In Fig. 2 the gas rate and density time traces are given for a series of H-mode shots which were performed with increasing gas rates at constant input power. With increasing gas rate the core density first increases and then saturates. Fig. 2 also shows that "negative ELMs" develop at high density, indicating detachment [7, 8].

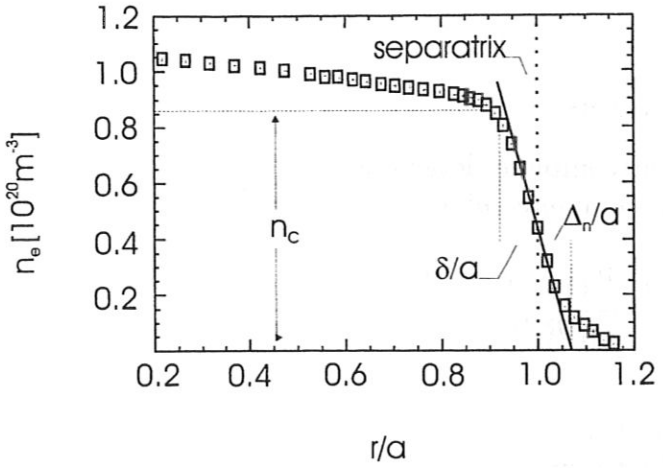

FIG. 3. *Typical density profile in a high density H-mode discharge. The gradient is constant in the pedestal and near the separatrix parts of the SOL and flat inside the pedestal. $\delta \approx \Delta_n$. (Example taken from ASDEX-Upgrade which is better diagnosed in this respect.)*

As an additional empirical element we use the observation that density gradients are constant in the pedestal and SOL regions and, in particular, do not jump at the separatrix as is illustrated by Fig. 3 which is representative of similar plots from a variety of machines. As regards the SOL, this statement is of course not literally true, especially in the outer part of the SOL. However, it is valid within the power fall off length, i.e., in the first few millimeters of the SOL, which is sufficient for the forthcoming argument (see Sec. 3). With this feature we get a simple relation between separatrix and pedestal density:

$$n_C = \frac{\delta + \Delta_n}{\Delta_n} n_S \tag{1}$$

Here subscripts $_C$ and $_S$ denote pedestal and separatrix quantities, respectively, δ is the pedestal width and Δ_n is the density fall off length. n_S and Δ_n in Eq. (1) are provided by the model of Ref. 3. For δ we make the simplest possible assumption $\delta \simeq const$ and take the actual value from experiment. This is, at least for JET, a well justified assumption [1].

In Eq. (1) n_C has to be interpreted as some kind of ELM cycle average (see Fig. 1 b)). Normally the variation of n_C during an ELM is small, so that the exact definition of this average is no matter of concern. However, there are parameter ranges where this approximation is no longer justified (see below). In that case our simple approach has to be replaced by a more refined description of the pedestal and outer core regions.

At detachment Δ_n becomes rather large and one has typically $\delta \approx \Delta_n$ (see Fig. 3). Then the approximation $(1 + z)/z \simeq 2(1/z)^{1/2}$, where $z = \Delta_n/\delta$, is quite good. It results in

$$n_C = 2\left(\frac{\delta}{\Delta_n}\right)^{1/2} n_S \tag{2}$$

which conveniently allows us to write the expression for the maximum density in power law form.

According to Figure 3 the peaking of n inside the pedestal is modest, even in the case of beam heating (and hence beam fuelling), thus justifying the approximation

$$\bar{n} \simeq n_C \tag{3}$$

which we will adopt throughout.

3. Modelling Considerations

In Ref. [3] scrape-off layer solutions at complete detachment were studied analytically and numerically. It was shown that at complete detachment and if Bohm-like transverse transport is adopted[1)]

$$n_S \propto \frac{q_\perp^x B_t^{5/16} (1 - f_{rad}^{SOL})^{x+1/16}}{(q_\psi R)^{11/16-x}} \tag{4}$$

holds, where R is the plasma major radius, q_ψ the safety factor (e.g., at the 95% flux surface), $q_\perp$ the mean power flux across the separatrix, f_{rad}^{SOL} the scrape-off layer impurity radiative fraction and B_t the toroidal field. The parameter x is related to the transverse neutral collisionality in the gas target and $x \geq -1/16$ holds. As was also shown in Ref. [3], $x \simeq -1/16$ should hold when complete detachment is achieved and we therefore conveniently confine the following discussion to this limit.

Also given in Ref. [3] is an expression for the (upstream) density decay length at complete detachment

$$\Delta_n \propto \frac{(q_\psi R)^{8/11} n_S^{7/11}}{q_\perp^{3/11} B_t^{7/11}} \tag{5}$$

(As in Ref. [3] we assume that transverse energy and particle transport are governed by the same mechanism, so that $\Delta_n \propto \Delta$, where Δ is the temperature fall-off length.)

Combining Eqs. (2), (3), (4) and (5), we get after some simple algebra

$$\bar{n} \propto \frac{q_\perp^{3/32} B_t^{17/32}}{(q_\psi R)^{7/8}} \tag{6}$$

for the core density at complete detachment.

The analytical considerations in Ref. [3] partly rely on dimensional considerations and do not provide the numerical coefficients in equations such as Eqs (4) and (5). However, since the scaling relations are well reproduced by 2-D code simulations, these coefficients can be determined by calibration with code results. For a typical case (JET MARK-I configuration, $\chi_{e,\perp} = D_{Bohm}$ $D_\perp = 0.2 D_{Bohm}$, $D_{Bohm} = cT_e/(16eB_t)$,[2)] $B_t = 2.4$T, $q_\psi = 3.6$, $R = 2.9$m, $a = 1.1$m, $P_{in} = P_{heat} - P_{rad}^{tot} = 2.4$MW) we get from the simulation $n_S = 3.43 \times 10^{19}\mathrm{m}^{-3}$ and $\Delta_n = 0.084$m, resulting in ($\delta = 0.07$m from the experiment)

$$\bar{n} = 4.14 \frac{q_\perp^{3/32} B_t^{17/32}}{(q_\psi R)^{7/8}} \tag{7}$$

where $\bar{n}$ is in $10^{20}\mathrm{m}^{-3}$, $q_\perp$ in $\mathrm{MW/m^2}$, B_t in T and R in m.

[1)] Different from Ref. [3] we now include SOL impurity radiation, which constitutes a straightforward extension.

[2)] The units are CGS units except where otherwise stated.

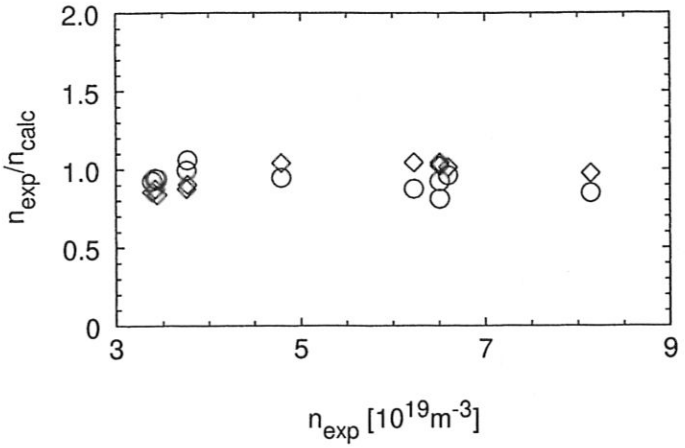

FIG. 4. $\bar{n}_{exp}/\bar{n}_{calc}$ *versus* $\bar{n}_{exp}$ *for JET highest density ELMy H-mode discharges of the 1995 MARK-I campaign. (○) Greenwald scaling. (◇) Proposed scaling according to Eq. (7). The experimental data cover discharge parameters in the ranges* $2.3MW \leq P_{heat} \leq 12.5MW$, $2.4 \leq q_\psi \leq 4.0$ *and* $1.0T \leq B_t \leq 2.5T$.

In Eq. (7) $q_\perp$ is the power flux flowing between ELMs across the separatrix. In describing empirical results the power dependence is typically given in terms of heating power P_{heat} which is related to $q_\perp$ according to

$$q_\perp = \frac{P_{heat}}{O_p}(1 - f_{rad}^{core})(1 - f_{ELM}) \tag{8}$$

where O_p is the plasma surface, f_{rad}^{core} $(= P_{rad}^{core}/P_{heat})$ the core radiative fraction and f_{ELM} the fraction of the power across the separatrix that is lost during ELMs. Typically f_{rad}^{core} and f_{ELM} increase with increasing power [9]. Therefore the P_{heat}-dependence is even weaker than the $q_\perp$-dependence. f_{rad}^{core} and f_{ELM} may also depend on B_t, q_ψ etc., but these dependencies would have to be extreme in order to become comparable with the explicit dependencies in Eq. (7).

Equation (7) provides the scaling of the maximum core density in ELMy H-mode as predicted by our model and constitutes our main result.

4. Comparison with Empirical Scalings and Experiment

We compare Eq. (7) with the empirical Greenwald scaling [10] and JET H-mode data. The Greenwald scaling, which provides a good description of H-mode density limit data of a variety of machines, can be written as (Hugill form [3])

$$\bar{n} = 1.59\frac{B_t}{Rq_\psi}g \tag{9}$$

where $\bar{n}$ is the maximum line averaged density in $10^{20}\mathrm{m}^{-3}$, B_t the toroidal field on axis in Tesla, R the major radius in meter, q_ψ the edge safety factor and g a factor that characterizes the plasma shape ($g = \mu_0 q_\psi R I_p/(2\pi a^2 B_t)$; in the crudest approximation $g \simeq \sqrt{s}$, where s is the plasma elongation). Apart from the B_t-dependence the proposed scaling Eq. (7) is rather close to the Greenwald scaling. The different B_t-dependence is not too much of a concern. For technical reasons the B_t-variation in density limit data sets is normally modest and insufficient to distinguish among the different scalings. (See also the discussion in Ref. [3].) This is illustrated by Fig. 4, which shows a comparison

of JET H-mode density limit data with values predicted by Eqs. (7) and (9). The data are a subset of the complete 1995 H-mode campaign, formed by discharges which meet the conditions (i) and (ii) of Sec. 1. Within the error bars both scalings describe the data equally well. It is impressive that the straightforward transport assumption made in the calibration runs that were used to evaluate the numerical coefficient in Eq. (7) provides basically the correct quantitative description.

In the more closed MARK-II divertor the maximum densities are systematically lower than in MARK-I. Also an increase of the density limit with increasing triangularity has been observed. Both effects are in the 10 to 15% range. The first effect is consistent with the observation of earlier detachment in MARK-II L-mode discharges [7, 11]. Increased triangularity leads to a widening of the ELM cycle (see Fig. 1) and this parameter range actually may constitute an example for the limitations of the simple picture underlying Eq. (1).

5. Summary and Conclusions

A model for the density limit of ELMy H-modes has been proposed which is set by divertor detachment between ELMs. A previously derived SOL model for the completely detached divertor, combined with experimental observations in the pedestal region, provides an explicit expression for the maximum achievable core density. The proposed density limit is, both in magnitude and scaling, close to the empirical Greenwald limit and is consistent with JET data.

The specific form of the proposed scaling depends on the model adopted for perpendicular transport. Various alternative models were considered in Ref. [3]. They all lead to additional size dependencies which clearly contradict existing data. Bohm based scalings along the lines of Ref. [3] and this paper, on the other hand, provide a consistent description of a variety of machines and regimes. This will be discussed in greater detail in a separate paper.

References

[1] LINGERTAT, J., et al., The Edge Operational Window and ELM Power Deposition in JET, in preparation.

[2] KAUFMANN. M., et al., Overview of ASDEX Upgrade Results, 16th IAEA Fusion Energy Conf., Montreal, 1996, paper F1-CN-64/O1-5.

[3] BORRASS, K., et al., Nuclear Fusion. **37** (1997) 523

[4] JANESCHITZ, G., et al., Plasma Phys. Control. Fusion **37** (1995) A19.

[5] BORRASS, K., Nucl. Fusion **31** (1991) 1035.

[6] BORRASS, K., et al., Nucl. Fusion **33** (1993) 63.

[7] MONK, R.D. et al, in Controlled Fusion and Plasma Physics (Proc. 24th Eur. Conf. Berchtesgaden, 1997), Vol. 21A, Part I, European Physical Society, Geneva (1997) 117.

[8] LOARTE, A., et al, Plasma Detachment in JET Mark-I Divertor Experiments, Report JET-P(97)03, JET Joint Undertaking, Abingdon, Oxfordshire (1997), to be published.

[9] HERRMANN, A., et al, in Controlled Fusion and Plasma Physics (Proc. 24th Eur. Conf. Berchtesgaden, 1997), Vol. 21A, Part IV, European Physical Society, Geneva (1997) 1417.

[10] GREENWALD, M., et al., Nucl. Fusion **28** (1988) 2199.

[11] BORRASS, K., et al, in Controlled Fusion and Plasma Physics (Proc. 24th Eur. Conf. Berchtesgaden, 1997), Vol. 21A, Part IV, European Physical Society, Geneva (1997) 1461.